JOURNAL OF ROCK MECHANICS

VOL. 8, NO. 2 , PP. 77-88.

https://doi.org/10.22034/IRSRM.2024.577088.1085

Development of a concentric-membrane cell for true triaxial stress testing of cylindrical rock samples

Mohsen Hedayati[1]; Nima Babanouri[2*]

1- M.Sc. Graduate, Department of Mining Engineering, Hamedan University of Technology, Hamedan, Iran.
2- Associate Professor, Department of Mining Engineering, Hamedan University of Technology, Hamedan, Iran.

Received: 05. July. 2024 Accepted: 21. September. 2024
(*Corresponding author: babanouri@hut.ac.ir)

Abstract

Rocks in nature are typically subjected to triaxial compressive stresses, clearly underscoring the importance of reliably measuring their true triaxial strength. However, true triaxial loading testing of rocks, mainly performed on cubic samples, still faces many challenges, such as an intricate sample preparation process and costly setup. This study presents a cell designed to apply true triaxial loads to rock cores using the conventional compression testing apparatus. The use of cylindrical specimens simplifies sample preparation, ensures compatibility with existing core drilling methods, and allows for more efficient replication of in-situ stress conditions in rock formations while avoiding stress concentration issues commonly observed at the corners of cubic specimens. The design of the cell is based on two concentric membranes. The annulus space between the membranes is divided into four 90-degree sectors, three of which are filled with steel plates, while the fourth is filled with hydraulic fluid. Each principal radial stress is provided by a separate hydraulic pump, and the axial stress is applied by a hydraulic jack. This study reports the results of 15 true triaxial tests on similar concrete samples using the innovative cell and under different stress fields.

Keywords ***True triaxial strength; Cylindrical specimen; Cell design; Concentric membranes***

1- Introduction

Rocks below the ground are subjected to in-situ triaxial stresses, including maximum, intermediate, and minimum stresses. This highlights the importance of measuring rock strength under triaxial stress conditions. The triaxial compression test provides insights into rocks' elastic and plastic properties, such as Young's modulus, Poisson's ratio, cohesion, and internal friction angle. Reliable measurement of these parameters is crucial for geomechanical design. Hence, several efforts have been made to develop equipment for applying triaxial loads to rock specimens.

Karman's triaxial test, performed in 1911 using a cylindrical cell encompassing the specimen, offered simple equipment and easy sample preparation [1,2]. In Karman's cell, the intermediate principal stress and the minimum principal stress were considered equal. This test, called conventional triaxial or biaxial testing, does not simulate the three-dimensional state of stress since it neglects the effect of the intermediate principal stress on rock failure [3]. By performing tests on brittle rock samples, Boker (1915) observed that the compressive strength of these rocks significantly depends on the confining stress [4]. The difference between Mohr's envelopes in pressure and tensile under equal confining stress was investigated by Murrell (1965) and Handin et al. (1967) [6], sparking the development of apparatus incorporating the intermediate principal stress in triaxial tests [7].

True triaxial apparatus can be classified by loading systems into rigid platen type, flexible platen type, or mixed type [8,9]. In the rigid platen type, stress is applied to the rock specimen using rigid plates or pistons that directly contact the sample surface. Robertson (1956) [10] and Hoskins (1969) [11] used a relatively large hollow cylinder specimen, but their efforts were accompanied by challenges due to a compression gradient and a loss of uniform stress distribution. Handin et al. (1967) used a thinner hollow cylinder [6], however, this method was not widely adopted due to the complexities and time-consuming nature of sample preparation and testing [12]. Weigler and Becker (1961, 1963) used a rigid platen type, consisting of three pairs of pistons applying stress to the sample [13,14]. Furuzumi and Sugimoto (1986) modified this by using three single pressuring platens and three rigid fixed plates [15]. One challenge associated with this test is the potential for the sample to deviate from the center of loading. King et al. (1995) developed a device with six hydraulic jacks confining a cubic sample without deviation [16]. The plates pressuring the sample were slightly smaller to prevent corner effects.

In the flexible medium type, stress is applied through a flexible membrane to the specimen in at least two directions [17,18]. One flexible medium cell used 24 elastic tubes to apply the minimum or intermediate principal stresses [18]. Franklin and Hoek (1970) introduced Hoek's cell [19], developed to facilitate triaxial testing of cylindrical specimens by applying uniform confining stress through a single membrane and axial stress through spherical seatings. Hoek's cell gained much attention in laboratory investigations [20]. Hergat and Unrug (1976) performed in-situ triaxial tests to determine the ultimate strength of large rock samples from high depths [21]. AlSayed (2002) modified Hoek's cell for triaxial tests on hollow samples [22].

The mixed type, first introduced by Mogi (1967) [23], combines rigid and flexible types. Mogi's apparatus modified Karman's device, exerting σ_1 and σ_2 with lateral jacks and σ_3 through oil pressure for uniform stress transfer [9]. Tani et al. (2003) designed a device for measuring triaxial strength at borehole bottoms [24]. Further attempts aimed at cost reduction through down-hole experiments on smaller samples [25]. Taheri and Tani (2011) performed in-situ triaxial tests on large rock mass samples at shallow depths and small-scale samples at greater depths [26]. Barla et al. (2010) developed a servo-controlled triaxial apparatus capable of testing under different boundary conditions and monitoring axial and lateral displacements and stresses [27]. Suzuki (2012) studied large specimens (500 mm × 500 mm × 500 mm) with slightly larger plates (700 mm × 700 mm) [28]. Schwarzkopff et al. (2013) developed a cost-effective prototype based on King et al.'s cell with changeable plates [29]. Schwarzkopff et al. (2014) enhanced Hoek's cell with structural health monitoring to investigate rock crack propagation during tests [30]. Mortazavi and Atapour (2020) introduced a true triaxial stress loading and pore pressure applying apparatus, designed for large rock specimens [31].

In true triaxial testing, cubic samples are commonly used; however, they are prone to stress concentration at the corners, which can distort failure patterns. Cylindrical specimens offer smoother boundary transitions and eliminate sharp corners, leading to more representative stress distributions. Additionally, cylindrical cores are easier to prepare using standard coring tools, making them advantageous for both experimental consistency and practical application.

This paper deals with an integrated design of a cell for true triaxial loading of cylindrical rock specimens. The design of the cell is based on two concentric membranes. Each annulus space is divided into four 90-degree sectors, three of which are filled with steel plates, and the other one is filled with a hydraulic fluid. Each principal radial stress is provided by a separate hydraulic pump, and the axial pressure is applied by a hydraulic jack. For evaluating the cell, 15 concrete

samples were produced and subjected to the true triaxial test.

2- Triaxial testing cell design

The objective was to modify Hoek's cell to apply different confining pressures to a cylindrical specimen. A top view of the initial design is illustrated in Figure 1. As shown, the design incorporates two concentric membranes. Each annular space is divided into four 90-degree sectors, two of which are filled with steel plates, and the other two with hydraulic fluid.

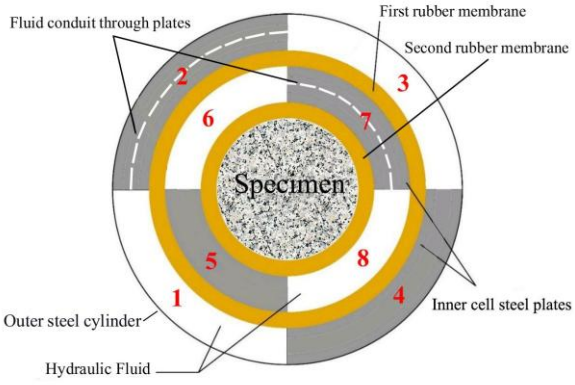

Figure 1. Top view of cell components in initial design

The hydraulic pressure in sectors #1 and #3 is transferred to the specimen via steel plates #5 and #7, respectively. To ensure uniform pressure in sectors #1 and #3, a conduit through steel section #2 was included.

A different confining pressure is applied to the specimen through the hydraulic fluid in sections #6 and #8, perpendicular to the first confining pressure. Similarly, a conduit through steel section #7 ensures equal pressure in sections #6 and #8. Each of the confining stresses is supplied by a separate hydraulic jack connected to sectors #1 and #8, respectively. A three-dimensional model of the cell, along with two-dimensional views, was prepared (Figures 2 and 3).

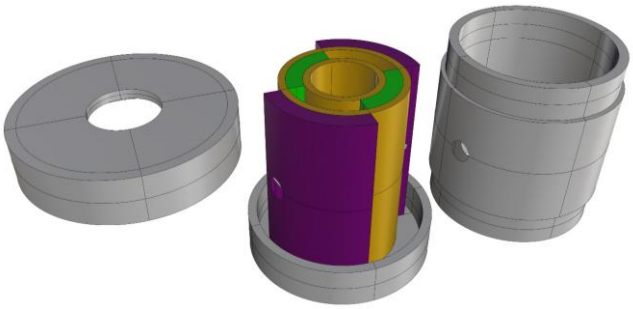

Figure 2. Three-dimensional model of cell components in initial design

A prototype of the triaxial cell was constructed using epoxy resin to realize the design (Figure 4). To prevent the plates inside the cell from moving due to fluid pressure, knobs were included on the outer wall of the plates. The prototype revealed a primary constraint: drilling conduits in sections #2 and #7 was challenging due to the curvature and low thickness of the steel plates.

Consequently, modifications were made to the initial design to eliminate the need for drilling in the steel sections. Additionally, the number of sealing interfaces was minimized in the modified design. Figure 5 presents a top view of the cell in the final design. In this design, the fluid pressure in sector #1 is transmitted to the specimen through steel sector #5. Conversely, an equal reaction force is applied to the specimen through steel sector #7. Similarly, the other confining pressure is applied to the specimen via the fluid pressure in section #8, and its reaction force is applied through steel sector #6. Figures 6 and 7 illustrate a three-dimensional model of the cell and its two-dimensional views.

A prototype of the triaxial cell was constructed using epoxy resin to realize the design (Figure 4). To prevent the plates inside the cell from moving due to fluid pressure, knobs were included on the outer wall of the plates. The prototype revealed a primary constraint: drilling conduits in sections #2 and #7 was challenging due to the curvature and low thickness of the steel plates.

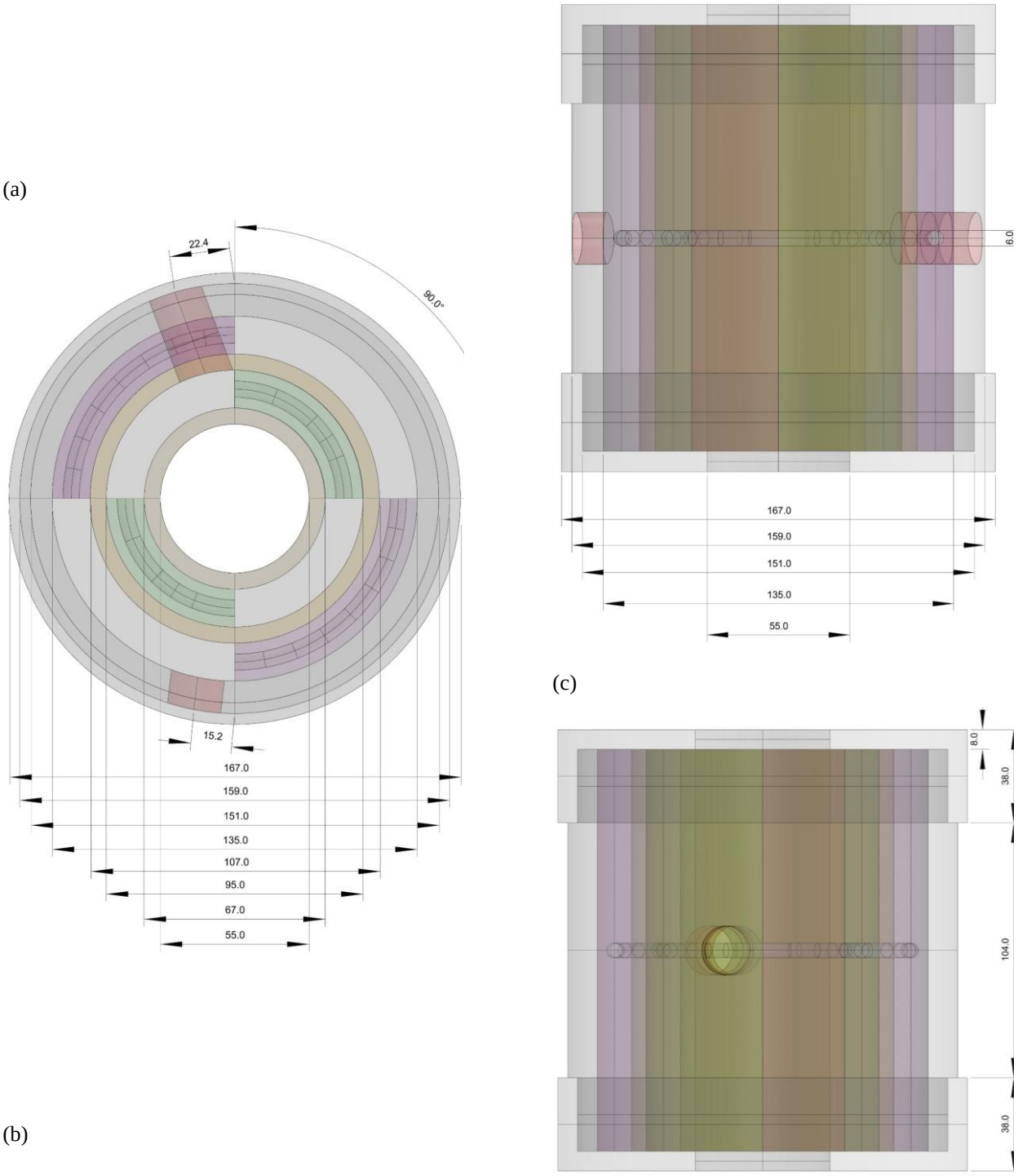

Figure 3. Initial design of triaxial cell (a) top view, (b) right view, (c) front view

Figure 4. Prototype of cell constructed using epoxy resin

Consequently, modifications were made to the initial design to eliminate the need for drilling in the steel sections. Additionally, the number of sealing interfaces was minimized in the modified design. Figure 5 presents a top view of the cell in the final design. In this design, the fluid pressure in sector #1 is transmitted to the specimen through steel sector #5. Conversely, an equal reaction force is applied to the specimen through steel sector #7. Similarly, the other confining pressure is applied to the specimen via the fluid pressure in section #8, and its reaction force is applied through steel sector #6. Figures 6 and 7 illustrate a three-dimensional model of the cell and its two-dimensional views.

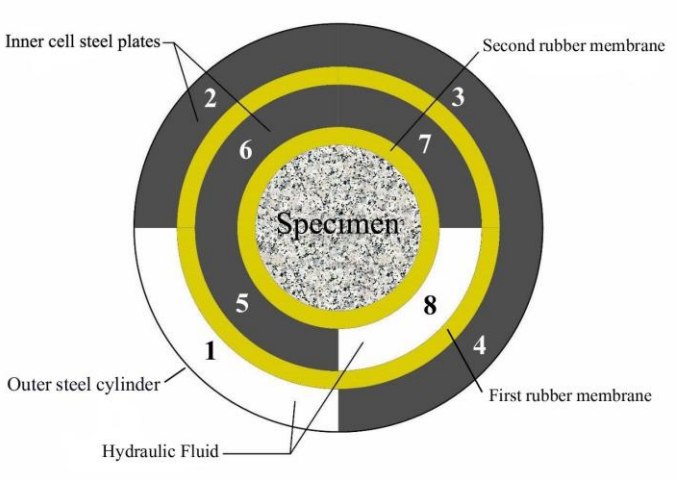

Figure 5. Top view of cell components in final design

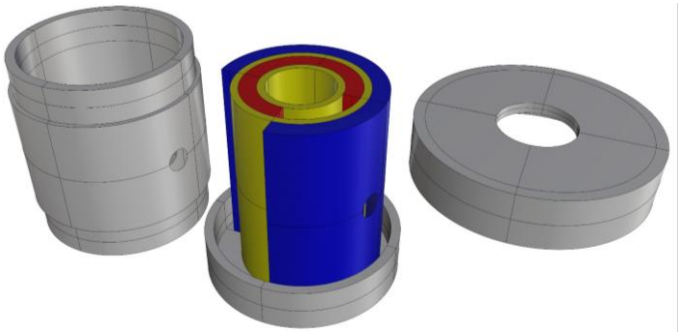

Figure 6. Three-dimensional model of cell components in final design

3- Construction of the cell

The cell was constructed according to the finalized design. Seamless tubes of varying thicknesses were utilized for the body and internal steel sectors. A polymer tube was employed for both rubber membranes. The outer cylinder was drilled to facilitate the connection of hydraulic jacks to sector #1 (see Figure 5). Additionally, the outer cylinder, steel section #4, and the first inner membrane were drilled to connect a hydraulic jack to sector #8. Figure 8 presents a top view of the cell before sealing.

Layers of silicone, latex, and polyurethane were applied to seal the interface between the steel and internal sectors. Figure 9 displays the final product.

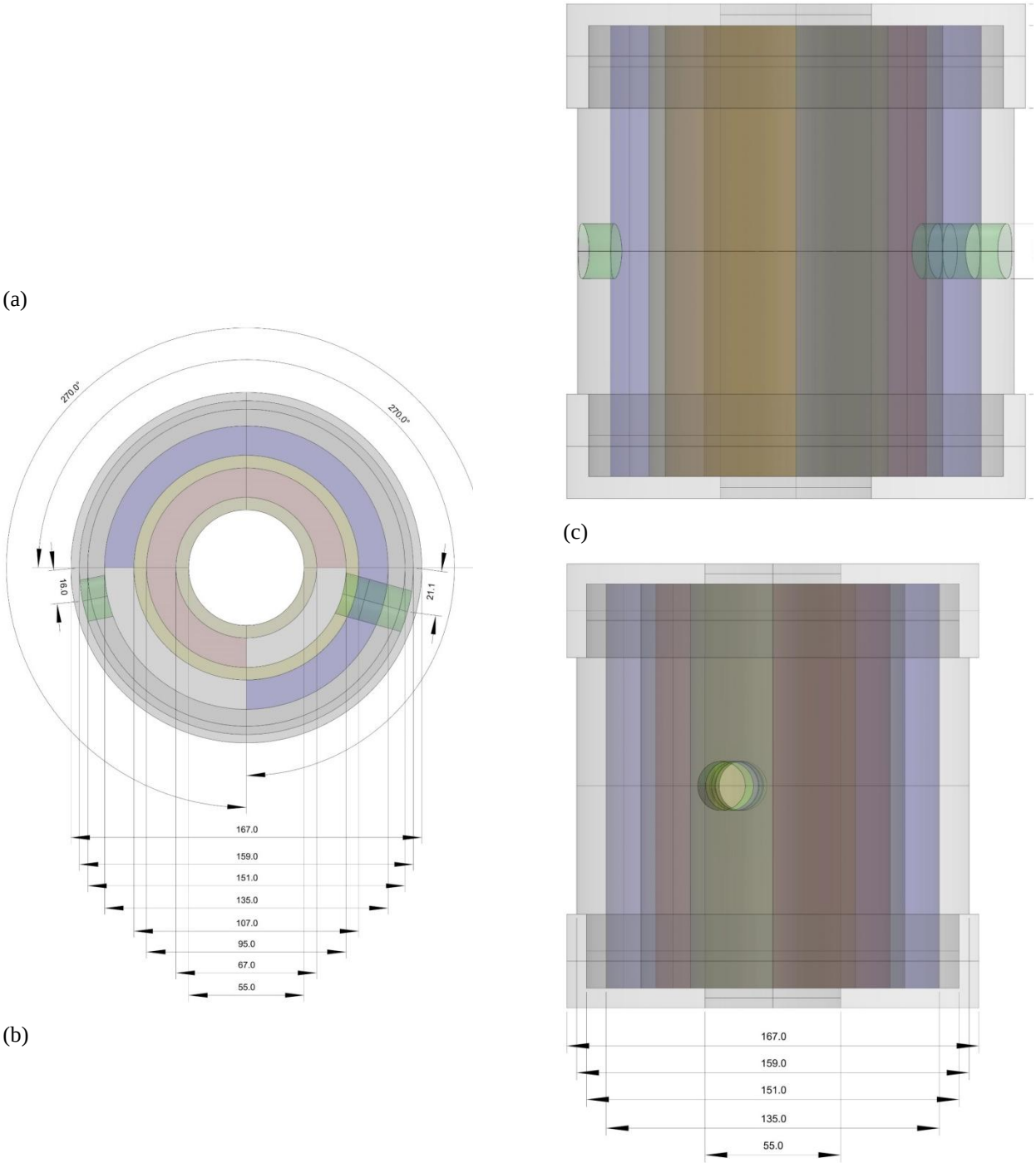

Figure 7. Final design of triaxial cell (a) top view, (b) right view, (c) front view

4- Laboratory testing

4-1- Sample preparation

To evaluate the cell, it was essential to test specimens with consistent mechanical properties. For this purpose, 15 concrete specimens with a diameter of 54

mm and a height of 110 mm were prepared (Figure 11). Concrete was chosen due to its mechanical consistency and suitability for verifying device functionality. The purpose of this study is not material-specific characterization but the evaluation of the cell's performance under varied triaxial stress states.
The concrete mixture comprised 75 wt% aggregates, 25 wt% cement, and water added at 40 wt% of the solid constituents.

4-2- True triaxial tests

To conduct the triaxial tests, the cell was connected to two hydraulic jacks that provided the confining pressures (Figure 12). A specimen was then placed inside the cell, and the upper and lower spherical seatings were positioned at the ends of the specimen.

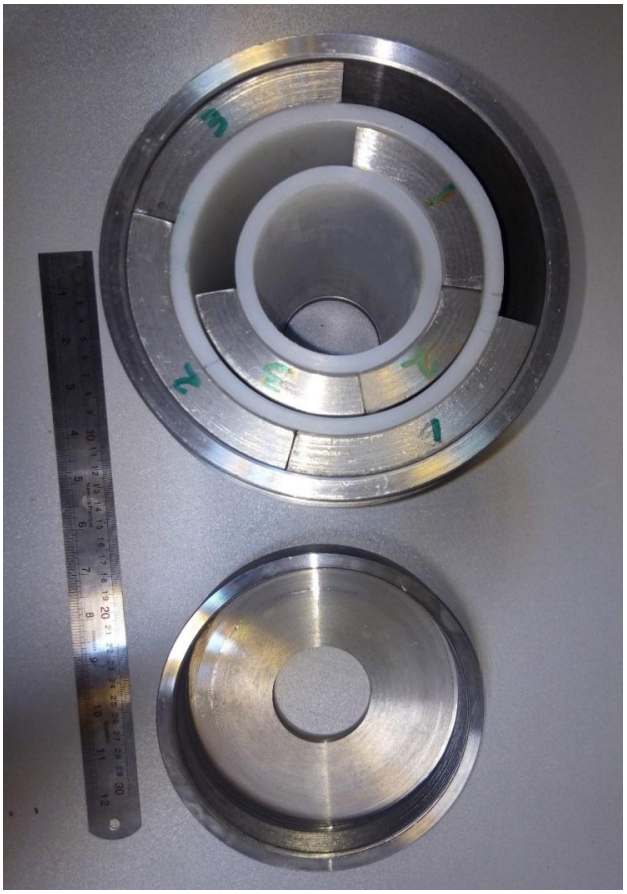

Figure 8. Top view of cell

Figure 9. Innovative triaxial cell

In the setup depicted in Figure 12, one hydraulic jack applied a pressure of 20 bar, while the other applied a pressure of 40 bar. A servo-controlled hydraulic jack was used to apply the axial stress (Figure 13). The axial load was increased gradually under load control at an approximate rate of 0.05 MPa/s, ensuring quasi-static conditions.

Figure 11. Concrete sample preparation

Figure 12. Connection of cell to hydraulic jacks applying different confining pressures.

Table 1 details the program and results of the tests performed on the concrete samples. Each stress condition was repeated three times to verify the repeatability of the results.

Table 1. Program and results of true triaxial tests

Test No.	σ_3 (MPa)	σ_2 (MPa)	σ_1 (MPa)
1, 2, 3	0.0	0.0	32.8, 33.1, 33.3
4, 5, 6	0.5	2.0	35.6, 34.6, 35.0
7, 8, 9	1.0	2.5	35.9, 36.6, 36.2
10, 11, 12	1.5	3.0	38.9, 39.4, 37.6
13, 14, 15	2.0	4.0	41.9, 39.7, 42.1

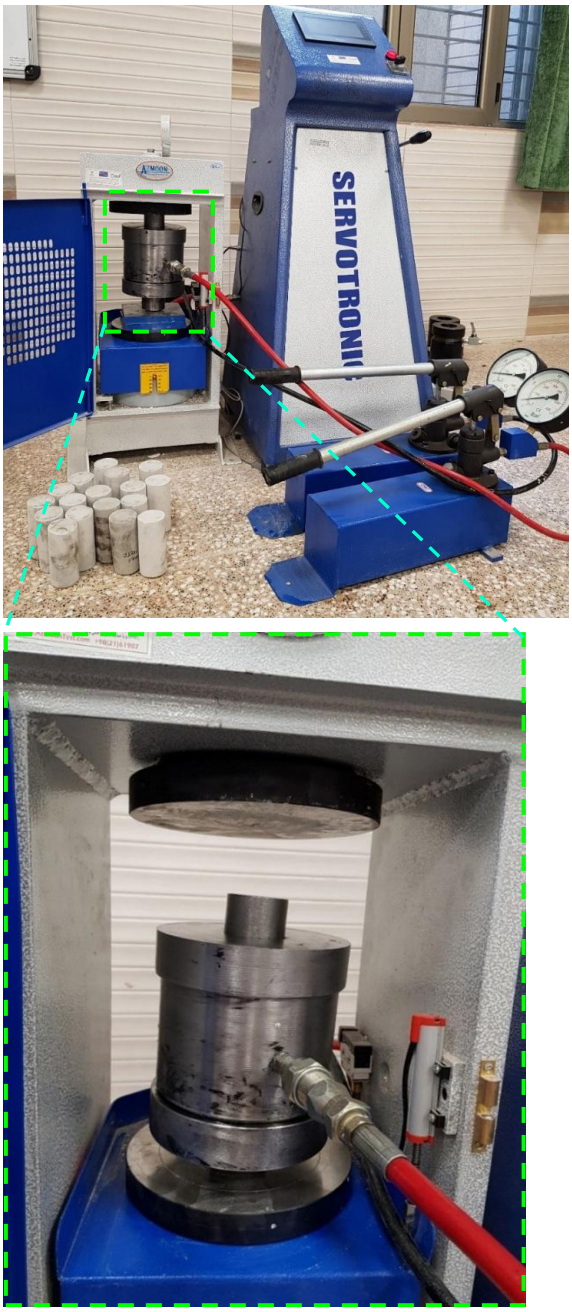

Figure 13. The setup of true triaxial test using developed cell

When interpreting data from true triaxial tests where $\sigma_2 \neq \sigma_3$, the Mogi-Coulomb criterion can be applied to account for the effect of the intermediate principal stress. Al-Ajami and Zimmerman (2005) [32] proposed a failure criterion that combines the Mogi criterion (1971) [33] with the linear Mohr-Coulomb failure criterion, known as the Mogi-Coulomb criterion. This criterion establishes a linear relationship between the octahedral shear stress (τ_{oct}) and the mean

effective stress (σ_{m2}):

$$\tau_{oct} = a + b\sigma_{m2} \quad (1)$$

when,

$$\tau_{oct} = \frac{1}{3}\sqrt{(\sigma_1 - \sigma_2)^2 + (\sigma_1 - \sigma_2)^2 + (\sigma_1 - \sigma_2)^2} \quad (2)$$

$$\sigma_{m2} = \frac{\sigma_1 + \sigma_3}{2} \quad (3)$$

The material constants a and b are related to the internal friction angle (ϕ) and cohesion (c) as follows:

$$a = \frac{2\sqrt{2}}{3} c \cos(\phi) \quad (4)$$

$$b = \frac{2\sqrt{2}}{3} c \sin(\phi) \quad (5)$$

Figure 14 presents the τ_{oct} versus σ_{m2} scatter plot of the true triaxial test results, along with the fitted Mogi-Coulomb criterion ($R^2 = 0.96$). Based on this criterion, the values of ϕ and c for the specimens were calculated to be 32.74° and 8.77 MPa, respectively.

The linear relationship observed in Figure 14 indicates that the shear strength of the samples increases proportionally with the mean effective stress, which aligns with the theoretical expectations of the Mogi-Coulomb criterion. However, it should be noted that this analysis primarily captures the macroscopic failure behavior without detailing localized failure planes or fracture mechanisms. Additionally, the data points demonstrate consistent repeatability across different stress states, further validating the reliability of the developed cell for capturing true triaxial strength parameters.

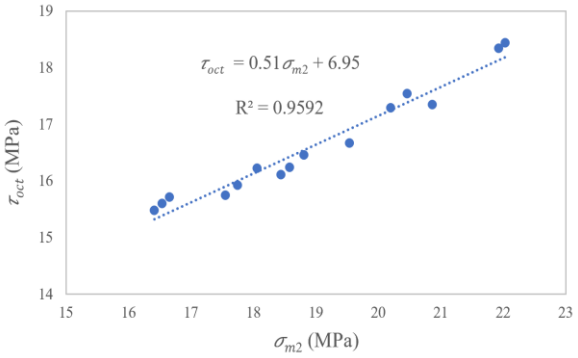

Figure 14. Values of τ_{oct} versus σ_{m2} along with fitted Mogi-Coulomb criterion

5- Conclusions

Since true triaxial testing was introduced to measure the ultimate strength of rocks, different cells have been developed for this purpose, almost all of which used cubic specimens that are difficult to prepare. In addition, these cells and their loading equipment are mostly expensive. The cell designed in this research allows for the application of different confining pressures in three orthogonal directions, facilitating a simple simulation of in-situ stress conditions on rock cores.

The cell was developed based on two concentric rubber membranes. Each annulus space was divided into four 90-degree sectors, three of which would be filled with steel plates, and fourth with hydraulic fluid.

The experimental phase involved the preparation of 15 concrete specimens with identical mechanical properties to ensure consistency in the test results. These specimens were subjected to varying confining pressures using the developed triaxial cell. The setup, including the connection of the cell to hydraulic jacks and the application of axial stress using a servo-controlled hydraulic jack, was executed to simulate true triaxial stress conditions.

The results of the true triaxial tests were interpreted using the Mogi-Coulomb criterion, which incorporates the effect of the intermediate principal stress. The high R^2 value of 0.96 indicates a strong correlation between the experimental data and the fitted Mogi-Coulomb criterion. The calculated values of internal friction angle and cohesion for the specimens, 32.74° and 8.77 MPa respectively, are consistent with the expected mechanical properties of concrete.

The cell designed in this research benefits from an integrated and cost-effective design that is compatible with simple equipment and specimens used in conventional triaxial tests.

Further studies are recommended to include numerical modeling to analyze the stress distribution within the developed cell and to optimize its design. In addition, experimental tests on a variety of real rock specimens are suggested to comprehensively evaluate the device's performance under different geomechanical conditions.

References

[1] F. Deák, P. Ván, B. Vásárhelyi, Hundred years after the first triaxial test, Periodica Polytechnica Civil Engineering. 56 (2012) 115–122. https://doi.org/10.3311/pp.ci.2012-1.13.

[2] T. V Karman, Festigkeitsversuche unter allseitigem Drunk, Z. Ver. Deu. Ing. 55 (1911) 1749.

[3] T. Esaki, T. Kimura, Mechanical Behavior Of Rocks Under Generalized High Stress Conditions, ISRM International Symposium.

(1989) 8.

[4] R. Boker, Die Mechanik der bleibenden Formanderung in kristallinisch aufgebauten Korpern, Ver. Dt. Ing. Mitt. Forsch. 175 (1915) 1–51.

[5] S.A.F. Murrell, The Effect of Triaxial Stress Systems on the Strength of Rocks at Atmospheric Temperatures, Geophysical Journal of the Royal Astronomical Society. 10 (1965) 231–281. https://doi.org/10.1111/j.1365-246X.1965.tb03155.x.

[6] J. Handin, H.C. Heard, J.N. Magouirk, Effects of the intermediate principal stress on the failure of limestone, dolomite, and glass at different temperatures and strain rates, Journal of Geophysical Research. 72 (1967) 611–640. https://doi.org/10.1029/JZ072i002p00611.

[7] M. Kwasniewski, X. Li, M. Takahashi, True triaxial testing of rocks, CRC Press, 2012.

[8] M. Takahashi, T. Narita, Y. Tomishima, R. Arai, Various loading systems for rock true triaxial compression test, Journal of the Japan Society of Engineering Geology. 42 (2001) 242–247.

[9] K. Mogi, Experimental rock mechanics, CRC Press, 2006.

[10] E.C. Robertson, Experimental study of the strength of rocks, Geological Society of America Bulletin. 66 (1955) 1275–1314.

[11] E.R. Hoskins, The failure of thick-walled hollow cylinders of isotropic rock, International Journal of Rock Mechanics and Mining Sciences & Geomechanics Abstracts. 6 (1969) 99–125. https://doi.org/10.1016/0148-9062(69)90030-8.

[12] R. Ulusay, International Society for Rock Mechanics., The ISRM suggested methods for rock characterization, testing and monitoring : 2007-2014, 2015.

[13] H. Weigler, G. Becker, Untersuchungen uber das Bruch-und Verformungsverhalten von beton bei Zweiachsiger Beanspruchung, Ernst, 1963.

[14] H. Weigler, G. Becker, Über das Bruch-und Verformungsverhalten von Beton bei mehrachsiger Beanspruchung, Der Bauingeneieur. 36 (1961) 390–396.

[15] M. Furuzumi, F. Sugimoto, Effect of Intermediate Principal Stress on Failure of Rocks and Failure Condition of Rocks under Multiaxial Stresses, Journal of the Japan Society of Engineering Geology. 27 (1986) 13–20.

[16] M.S. King, N.A. Chaudhry, A. Shakeel, Experimental ultrasonic velocities and permeability for sandstones with aligned cracks, International Journal of Rock Mechanics and Mining Sciences And. 32 (1995) 155–163. https://doi.org/10.1016/0148-9062(94)00033-Y.

[17] J.P.M. Hojem, The design and construction of a tiaxial and polyaxial cell fortesting rock materials, S. Afr Mech. Engr. 18 (1968) 57–61.

[18] B.G.D. Smart, A true triaxial cell for testing cylindrical rock specimens, in: International Journal of Rock Mechanics and Mining Sciences and Geomechanics Abstracts, 1996: p. 67A.

[19] J.A. Franklin, E. Hoeck, Developments in triaxial testing technique, Rock Mechanics Felsmechanik Mécanique Des Roches. 2 (1970) 223–228. https://doi.org/10.1007/BF01245576.

[20] X. Li, L. Shi, B. Bai, Q. Li, D. Xu, X. Feng, True-triaxial testing techniques for rocks—state of the art and future perspectives, True Triaxial Testing of Rocks. (2012) 3–18. https://doi.org/10.1201/b12705.

[21] G. Herget, K. Unrug, In situ rock strength from triaxial testing, International Journal of Rock Mechanics and Mining Sciences And. 13 (1976) 299–302. https://doi.org/10.1016/0148-9062(76)91828-3.

[22] M.I. Alsayed, Utilising the Hoek triaxial cell for multiaxial testing of hollow rock cylinders, International Journal of Rock Mechanics and Mining Sciences. 39 (2002) 355–366. https://doi.org/10.1016/S1365-1609(02)00030-8.

[23] K. Mogi, Effect of the Intermediate Principal Stress on Rock Failure, Journal of Geophysical Research. 72 (1967) 5117–5131.

[24] K. Tani, T. Nozaki, S. Kaneko, Y. Toyo-oka, H. Tachikawa, Down-hole triaxial test to measure average stress-strain relationship of rock mass, Soils and Foundations. 43 (2003) 53–62.

[25] A. Taheri, K. Tani, Development of an apparatus for down-hole triaxial tests in a rock mass, International Journal of Rock Mechanics and Mining Sciences. 45 (2008) 800–806. https://doi.org/10.1016/j.ijrmms.2007.09.005.

[26] A. Taheri, K. Tani, In-Situ Triaxial Test Method For Rock Masses–Apparatus Description And Testing Procedure, in: Geotechnical Engineering For Disaster Mitigation And Rehabilitation And Highway Engineering 2011: Geotechnical and Highway Engineering—Practical Applications, Challenges and Opportunities (With CD-ROM),

World Scientific, 2011: pp. 475–480.

[27] G. Barla, M. Barla, D. Debernardi, New triaxial apparatus for rocks, Rock Mechanics and Rock Engineering. 43 (2010) 225–230. https://doi.org/10.1007/s00603-009-0076-7.

[28] K. Suzuki, Study of the failure and deformability of jointed rock masses using large rock block specimens, True Triaxial Testing of Rocks. 4 (2012) 61.

[29] A.K. Schwarzkopff, S. Priest, N. Melkoumian, J.A. Egudo, Design and fabrication of a low cost true triaxial cell for testing multiple size specimens, 2013.

[30] A.K. Schwartzkopff, N.S. Melkoumian, S.D. Woithe, Design Improvements for a True Triaxial Cell to Monitor Initiation and Propagation of Damage and Body Cracks during Testing BT - Mine Planning and Equipment Selection, in: C. Drebenstedt, R. Singhal (Eds.), Springer International Publishing, Cham, 2014: pp. 551–560.

[31] H. Atapour, A. Mortazavi, Performance Evaluation of Newly Developed True Triaxial Stress Loading and Pore Pressure Applying System to Simulate the Reservoir Depletion and Injection. Geotechnical Testing Journal 43 (2020): 701–719.

[32] A.M. Al-Ajmi, R.W. Zimmerman, Relation between the Mogi and the Coulomb Failure Criteria. International Journal of Rock Mechanics and Mining Sciences 42 (2005): 431–39.

[33] K. Mogi, Fracture and Flow of Rocks under High Triaxial Compression. Journal of Geophysical Research 76 (1971): 1255–69.

نشریه‌ی مکانیک سنگ
JOURNAL OF ROCK MECHANICS
دوره هشتم، شماره۲، تابستان ۱۴۰۳، صفحه ۷۷ تا ۸۸
https://doi.org/10.22034/IRSRM.2024.577088.1085

توسعه یک سلول با غشای هم‌مرکز برای آزمایش تنش سه‌محوره واقعی روی نمونه‌های سنگی استوانه‌ای

محسن هدایتی[1]؛ نیما بابانوری [2*]

۱- دانش‌آموخته کارشناسی ارشد، گروه مهندسی معدن، دانشگاه صنعتی همدان، همدان، ایران.

۲- دانشیار گروه مهندسی معدن، دانشگاه صنعتی همدان، همدان، ایران.

دریافت : ۱۴۰۳/۰۴/۱۵؛ پذیرش: ۱۴۰۳/۰۶/۳۱

(*نویسنده مسئول: babanouri@hut.ac.ir)

واژگان کلیدی

مقاومت سه‌محوره واقعی
نمونه استوانه‌ای
طراحی سلول
غشای هم‌مرکز

چکیده بلند فارسی

خلاصه

سنگ‌ها در طبیعت معمولاً تحت تنش‌های سه‌محوره قرار دارند، بنابراین اندازه‌گیری مقاومت سه‌محوره واقعی آن‌ها از اهمیت بالایی برخوردار است. با این حال، آزمایش‌های سه‌محوره واقعی روی سنگ‌ها، که عمدتاً روی نمونه‌های مکعبی انجام می‌شود، با چالش‌هایی مانند فرآیند پیچیده آماده‌سازی نمونه و هزینه‌های بالای تجهیزات مواجه است. در این مطالعه، یک سلول طراحی شده است که امکان اعمال بارهای سه‌محوره واقعی را روی نمونه‌های استوانه‌ای سنگ با استفاده از دستگاه‌های معمولی آزمایش فشار فراهم می‌کند. استفاده از نمونه‌های استوانه‌ای، فرآیند آماده‌سازی نمونه را ساده‌تر می‌کند، با روش‌های موجود حفاری مغزه سازگار است و امکان شبیه‌سازی کارآمدتر شرایط تنش درجا در سازندهای سنگی را فراهم می‌سازد، در حالی که از مشکلات تمرکز تنش که معمولاً در گوشه‌های نمونه‌های مکعبی مشاهده می‌شود، جلوگیری می‌کند. طراحی این سلول بر اساس دو غشای هم‌مرکز است که فضای بین آن‌ها به چهار بخش ۹۰ درجه تقسیم شده است. سه بخش از این فضا با صفحات فولادی پر شده و بخش چهارم با سیال هیدرولیک پر می‌شود. هر یک از تنش‌های اصلی شعاعی توسط یک پمپ هیدرولیک جداگانه تأمین می‌شود و تنش محوری نیز توسط یک جک هیدرولیک اعمال می‌شود. در این مطالعه، نتایج ۱۵ آزمایش سه‌محوره واقعی روی نمونه‌های بتنی مشابه با استفاده از این سلول نوآورانه و تحت شرایط تنش مختلف گزارش شده است.

مقدمه

سنگ‌ها در زیر زمین تحت تنش‌های سه‌محوره شامل تنش‌های حداکثر، متوسط و حداقل قرار دارند. این موضوع اهمیت اندازه‌گیری مقاومت سنگ تحت شرایط تنش سه‌محوره را نشان می‌دهد. آزمایش فشار سه‌محوره اطلاعاتی در مورد خواص الاستیک و پلاستیک سنگ‌ها، مانند مدول یانگ، نسبت پواسون، چسبندگی و زاویه اصطکاک داخلی ارائه می‌دهد. اندازه‌گیری قابل اعتماد این پارامترها برای طراحی‌های ژئومکانیکی ضروری است. بنابراین، تلاش‌های زیادی برای توسعه تجهیزات اعمال بار سه‌محوره روی نمونه‌های سنگی انجام شده است.

روش تحقیق

هدف این مطالعه، طراحی و توسعه یک سلول برای اعمال فشارهای سه‌محوره واقعی روی نمونه‌های استوانه‌ای سنگ است. طراحی سلول بر اساس دو غشای هم‌مرکز است که فضای بین آن‌ها به چهار بخش ۹۰ درجه تقسیم شده است. سه بخش از این فضا با صفحات فولادی پر شده و بخش چهارم با سیال هیدرولیک پر می‌شود. هر یک از تنش‌های اصلی شعاعی توسط یک پمپ هیدرولیک جداگانه تأمین می‌شود و تنش محوری نیز توسط یک جک هیدرولیک اعمال می‌شود. برای ارزیابی سلول، ۱۵ نمونه بتنی با خواص مکانیکی یکسان تهیه شد و تحت آزمایش‌های سه‌محوره واقعی قرار گرفت.

نتایج و بحث

نتایج آزمایش‌های سه‌محوره واقعی با استفاده از معیار Mogi-Coulomb تفسیر شدند. این معیار تأثیر تنش اصلی متوسط را در نظر می‌گیرد و رابطه خطی بین تنش برشی اکتاهدرال و تنش مؤثر متوسط را برقرار می‌کند. مقادیر زاویه اصطکاک داخلی و چسبندگی برای نمونه‌ها به ترتیب ۲۲/۷۴ درجه و ۸/۷۷ مگاپاسکال محاسبه شد. ضریب تعیین (R^2) برابر با ۰/۹۶ نشان‌دهنده تطابق خوب بین داده‌های آزمایشی و معیار Mogi-Coulomb است

نتیجه‌گیری

سلول طراحی شده در این پژوهش امکان اعمال فشارهای سه‌محوره واقعی را روی نمونه‌های استوانه‌ای سنگ فراهم می‌کند و شبیه‌سازی شرایط تنش درجا را ساده‌تر می‌کند. این سلول از طراحی یکپارچه و مقرون‌به‌صرفه برخوردار است و با تجهیزات ساده و نمونه‌های مورد استفاده در آزمایش‌های سه‌محوره معمولی سازگار است. نتایج این مطالعه می‌تواند به بهبود روش‌های آزمایشگاهی برای ارزیابی مقاومت سنگ‌ها تحت شرایط تنش سه‌محوره کمک کند.